

## CHAPTER VI

### HIGH PRESSURE STUDIES ON DISC LIKE MESOGENS

#### **1. Introduction:**

Since the discovery of liquid crystals in 1888, thousands of pure compounds have been found to exhibit thermo-tropic mesophases. The distinctive feature common to all of them is the rod like or the lath like shape of the molecule. Brooks and Taylor (1) described in 1965, the formation of intermediate phases consisting of large plate like molecules at relatively high temperature (450 C). These mesophases were found to occur during the carbonization of certain graphiteable substances such as petroleum and coal tar. However, these carbonaceous mesophases are rather complex materials composed of large molecules and certainly cannot be regarded as single component liquid crystalline substances. Recently Chandrasekhar et al (2, 3) discovered the existence of thermo tropic mesomorphism in pure compounds consisting of relatively simple disc-like molecules. The compounds investigated by them were benzene hexa-n-alkanoates which have molecular structure shown in figure 1. From thermodynamic, optical and X-ray studies they concluded that these mesophases form a new type of liquid crystalline structure as illustrated in figure 2 of Chapter I. The discs are stacked in columns with an irregular spacing, the different columns forming hexagonal array. Since this

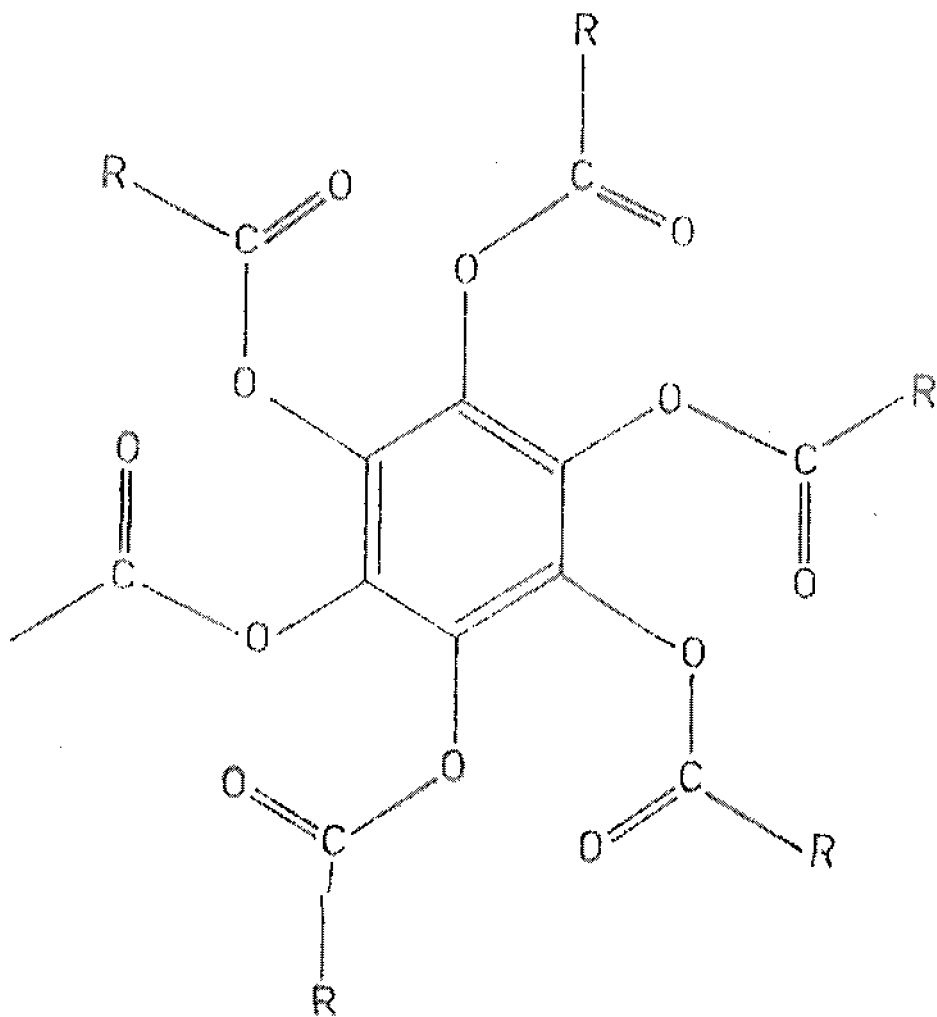


Figure 1: Molecular structure of disc-like mesogens

first observation of the disc like mesophase several other compounds have been synthesized which also show similar disc like mesophases (4-7). Recent X-ray investigations of Levelut (8) have confirmed the structure proposed by Chandrasekhar et al. These mesophases are termed as canonic or columnar mesophases or sometimes as discotic phases.

We have carried out a detailed investigation of the effect of pressure on the phase transitions in the sixth to the ninth homologues of the benzene hexa-n-alkanoates which we shall abbreviate as **BH<sub>n</sub>** for convenience. These are the first high pressure experiments on disc like mesogens.

## 2. Experimental:

The transition temperatures of the compounds at atmospheric pressure and the heats of transition (H) were obtained using Perkin-Elmer Differential Scanning Calorimeter (DSC – 2). These data are given in table I. The heats associated with both the solid-mesophase and the mesophase-isotropic transitions are relatively large and are of comparable magnitude in the BH7 – BH9 derivation. BH6 is a non-mesomorphic substance which, however, exhibits a solid-solid transition before the melting transition at atmospheric pressure. It is also seen from the table that H of the melting transition increases systematically from BH6 – BH9 derivatives, whilst H of the mesophase to isotropic transition shows a systematic decrease. Also in all these cases there is a strong super cooling of the isotropic at mesophase transition, the transition temperature obtained on the cooling mode being as different as 3.5 C from that obtained in the heating mode. This large super cooling is evidently related to the usually high H associated with the mesophase-isotropic transition.

The transition temperatures as a function of pressure were determined using the high pressure DTA cell (see chapter II). All the DTA runs except those in the case of BH9 were recorded in the heating mode only. In the case of BH9, which shows a monotropic mesophase at atmospheric pressure, the DTA runs were recorded in the cooling mode also.

## 3. Results and Discussion:

### a) Benzene-hexa-n-hexanoate (BH6)

As stated earlier, this compound is non-mesomorphic at atmospheric pressure, melting directly into an isotropic phase at 94.5 C, although there is a solid I – solid II transition at 75.5 C. The data obtained for this compound are given in table II and the

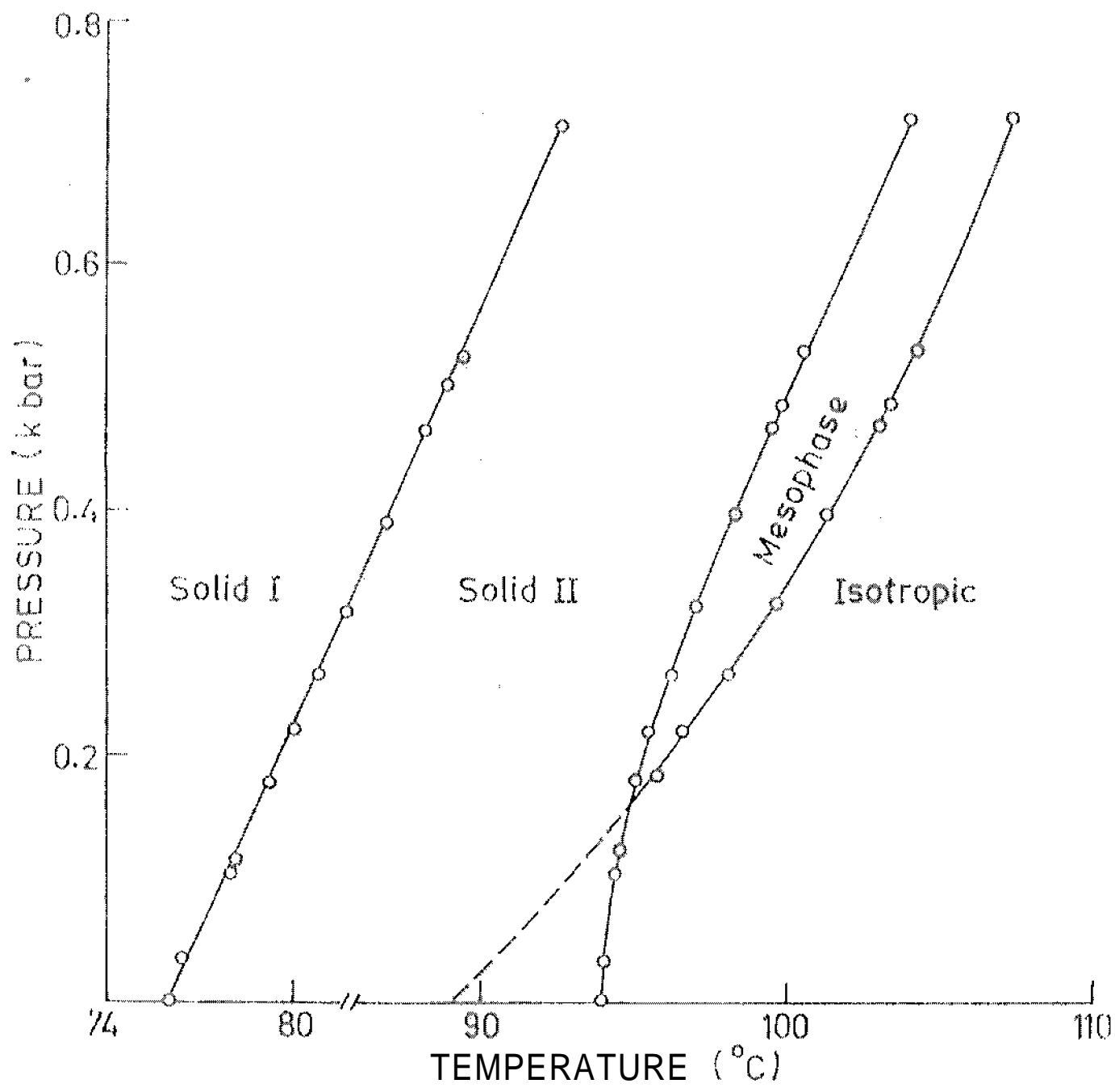


Figure 2: Phase diagram of benzene-hexa-n-hexanoate

P-T diagram is shown in figure 2. It is seen that the solid I – solid II phase boundary is linear throughout the pressure range studied. On the other hand, a most striking feature is observed with respect to solid II – isotropic mesophase. Initially up to a pressure of 180 bars, there is only the melting transition whose temperature

Increases with increase of pressure. But at a pressure of about 200 bars, the phase diagram forks, there now being two transitions, solid II – mesophase and mesophase – isotropic, separated by about 10 C. With further increase of pressure, the range of this pressure induced phase increase. Typical DTA runs showing just the solid-solid and melting transitions at a pressure of 150 bars is given in figure 3(a) while figure 3(b) gives the raw DTA run taken at a pressure of 300 bars showing the new pressure induced phase.

The possibility of inducing liquid crystallinity to non-mesomorphic compounds having rod like molecules by the application of pressure was first predicted theoretically by Chandrasekhar et al (9) who also confirmed such a behaviour experimentally. (10) Subsequently similar observations have been made in other compounds by Shashidhar (11) and Cladis et al. (12) The compounds selected in all the above cases were such that the lower homologues were non-mesomorphic while the higher ones showed mesomorphism at atmospheric pressure.

Considering our results on BH6 in the light of the above observation, it is very likely that the new induced phase beyond a pressure of 200 bars is also a disc like mesophase. The triple point in this case is at  $160 \pm 0.08$  bars,  $94.5 \pm 1.5$  C. The extrapolation of the mesophase-liquid transition line of the P-T phase diagram (figure 2) leads to a virtual monotropic transition at 89 C. This value for the virtual mesophase-isotropic transition temperature of BH6 is in excellent agreement with that obtained from miscibility studies carried out by Billard and Sadashiva (13). They have evaluated the isobaric phase diagram for the mixture of BH6 and BH7 compounds for different concentrations (Figure 4). The dotted lines in this figure are the extrapolation of the observed spindle for the enantio-isotropic mesophase-liquid transition. This yields a virtual mesophase-liquid transition at 89 C for BH6.

The  $dT/dP$  evaluated from the initial slopes of the phase boundaries of the experimental phase diagram are 17.4 C/kbar for the solid I – solid II and 6.1 C/kbar for the solid II – isotropic transitions. Further the  $dT/dP$  values evaluated near the pressure induced phase – isotropic transitions are 6.8 C/kbar and 14.8 C/kbar respectively. We shall discuss these values in detail later.

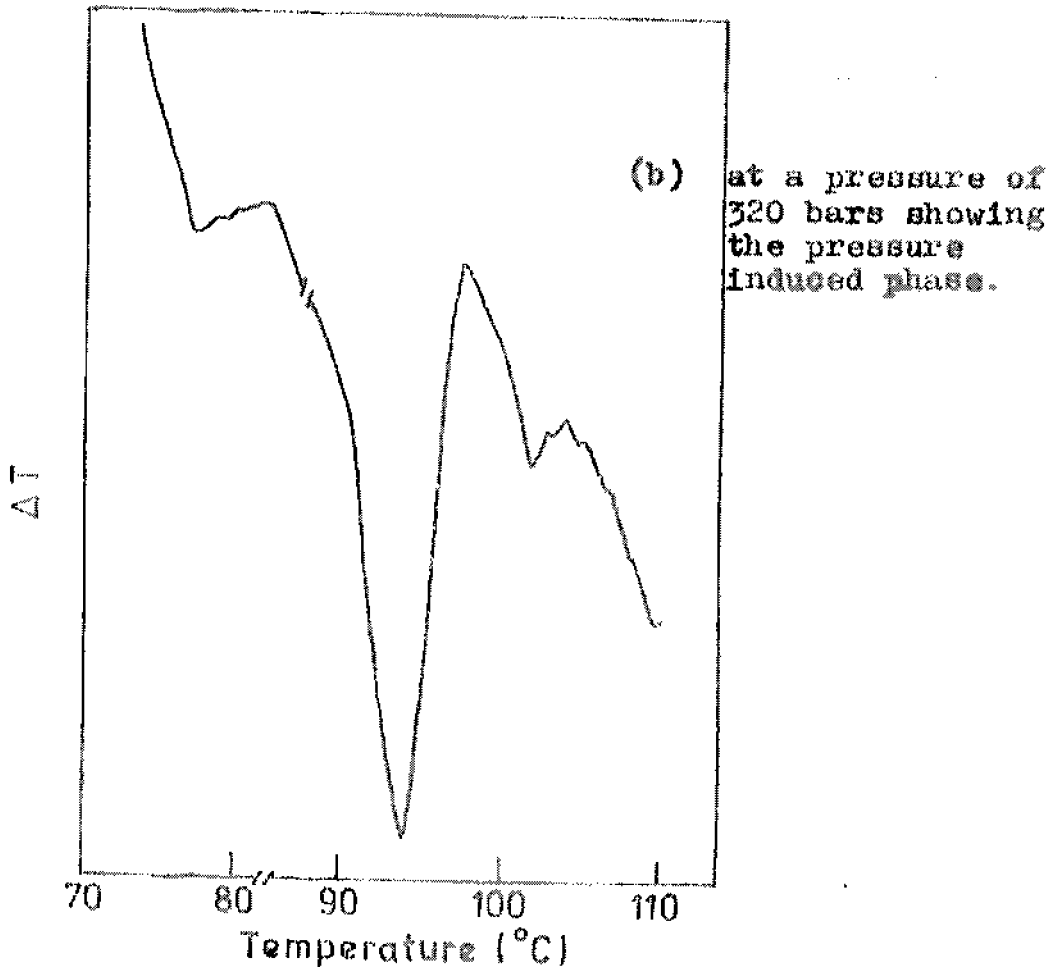
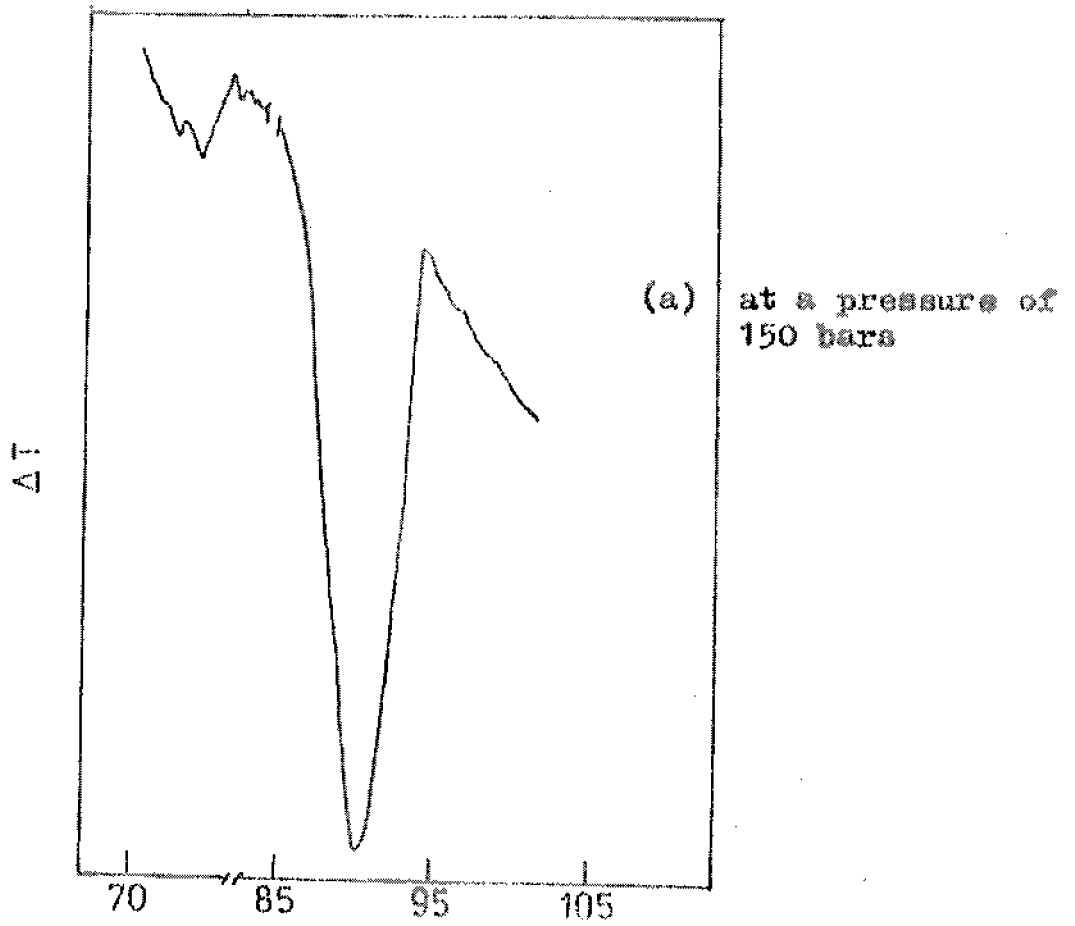


Figure 3: Raw DTA traces of BH6

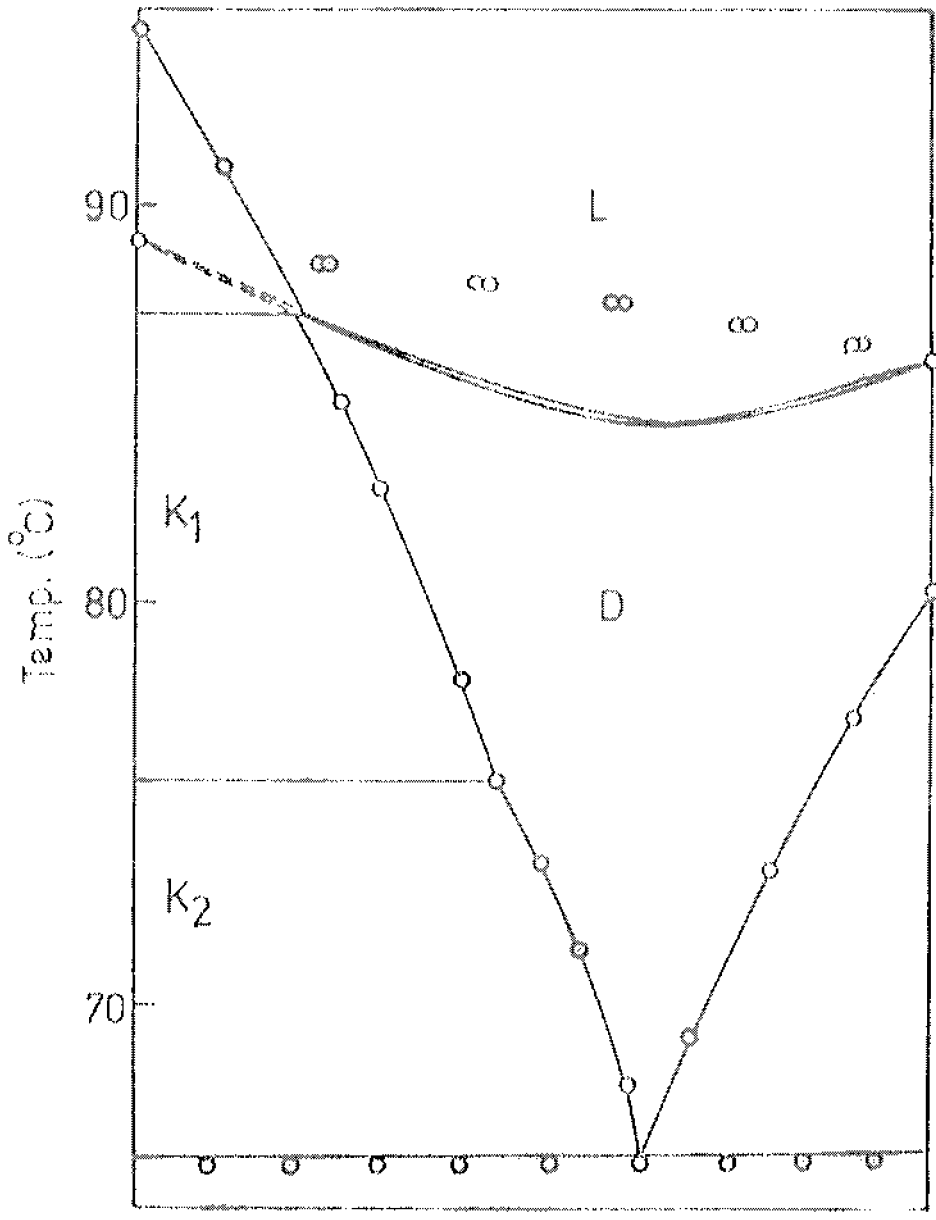


Figure 4: Isobaric phase diagram for the mixtures of BH5 and BH6 (after Hillard and Sudashiva (13)).

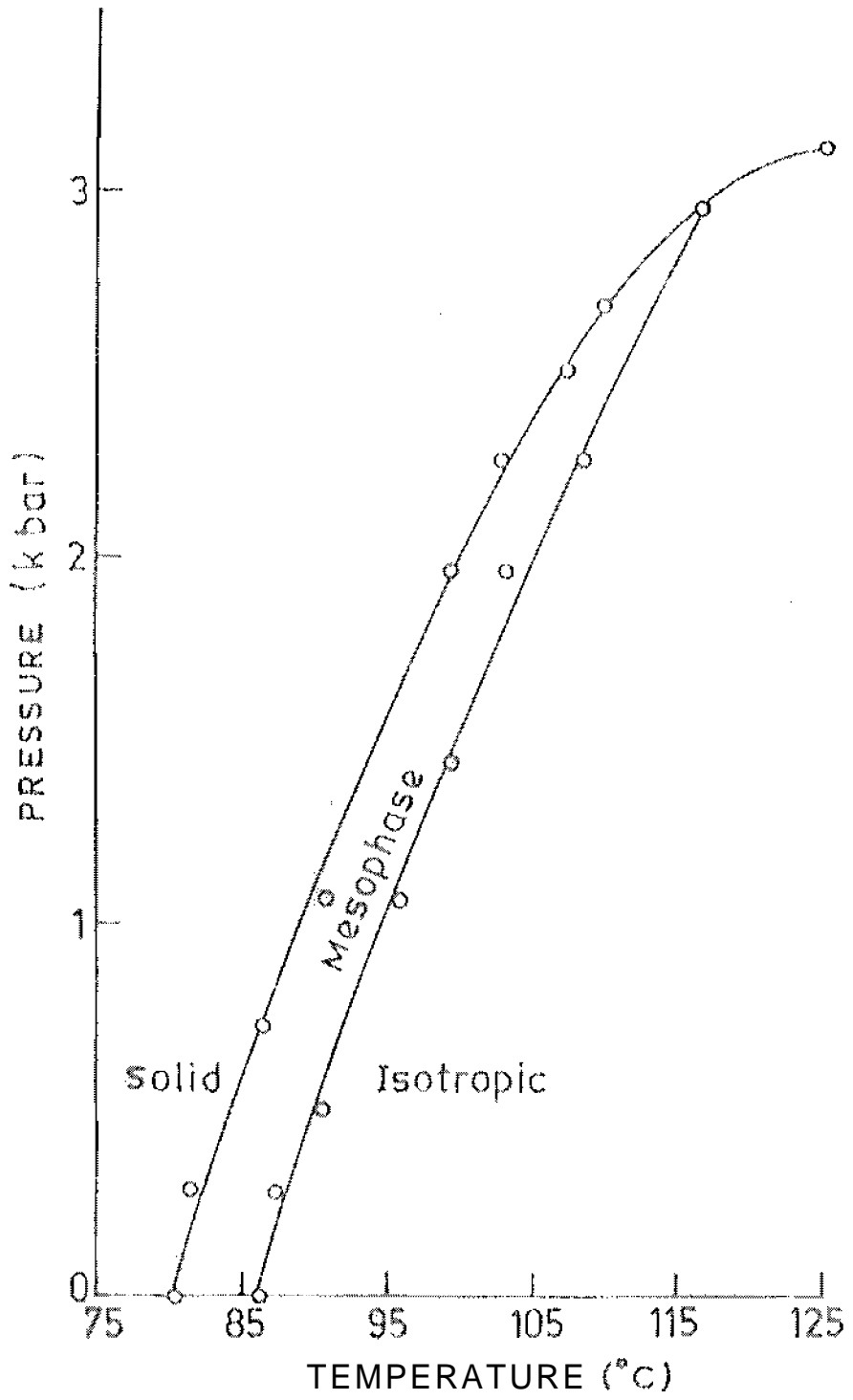


Figure 5: Phase diagram of benzene-hexa-n-heptanoate



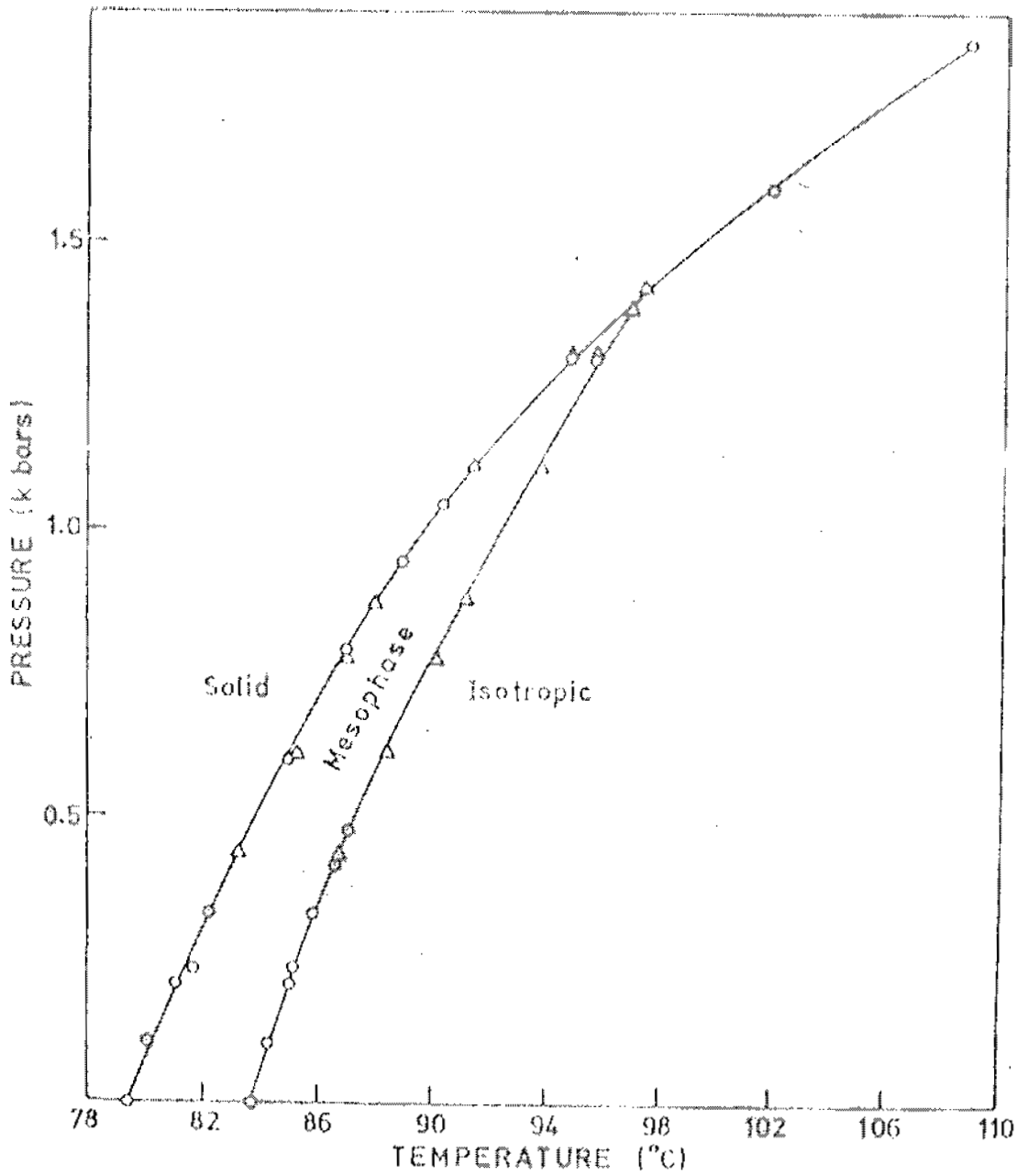


Figure 6: Phase diagram of benzene-hexa-n-octanoate. The  $\Delta$  and  $\circ$  represent two independent sets of measurements.

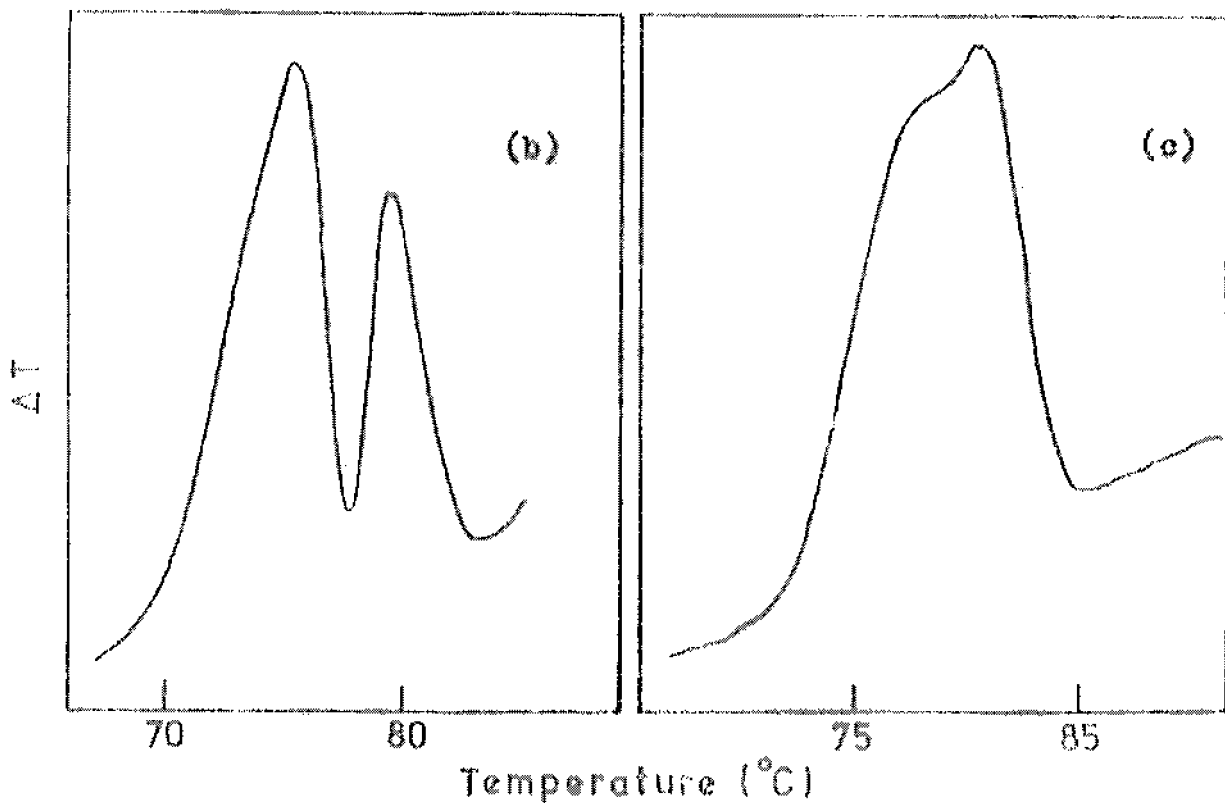
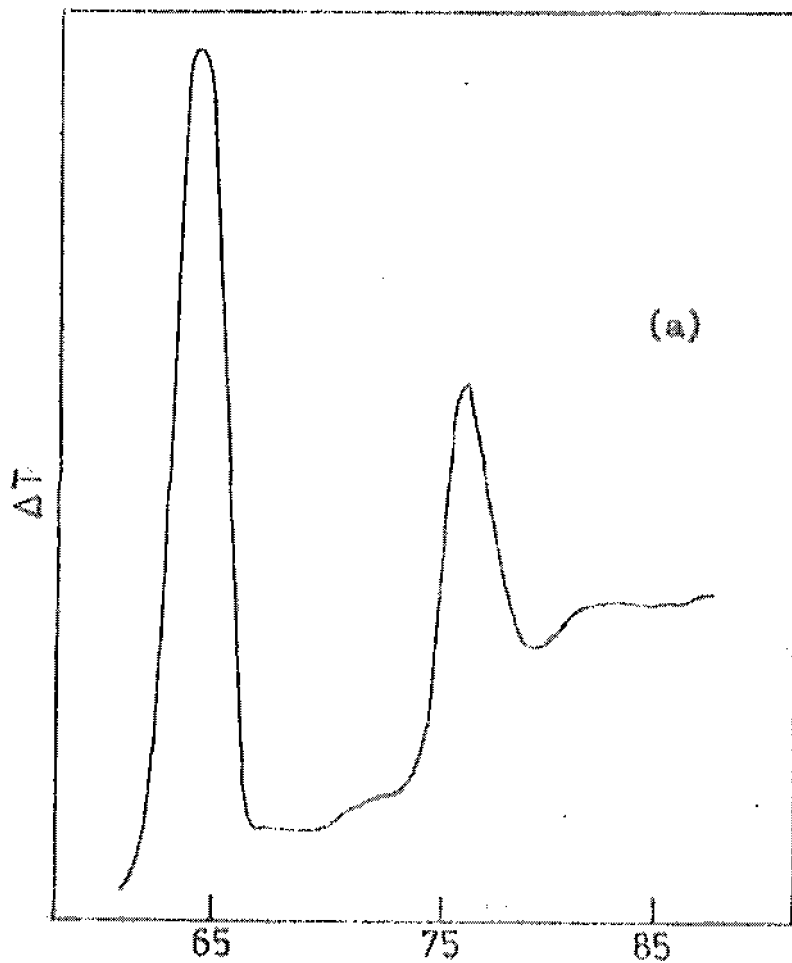


Figure 7: Raw DTA traces of BH8 (a) at atmospheric pressure, (b) at a pressure of 1.2 kbars, (c) at a pressure of 1.4 kbars.

b) Benzene hexa-n-heptanoate and octanoate

Both these compounds exhibit enantiotropic mesophases at atmospheric pressure. The data for these compounds are given in tables III and IV and the phase diagrams in figures 5 and 6 respectively. Both the phase diagrams exhibit similar features. In the case of BH8 which has a narrow mesomorphic range of about 3.6 C at atmospheric pressure, the range decreases with increase of pressure (see figure 7a and 7b). On further increase of pressure the two transition lines begin to converge and finally coalesce resulting in a single transition with much larger entropy of fusion (figure 7c). Therefore the mesophase in BH8 is fully bounded with a resultant solid – mesophase – isotropic triple point at  $1.43 \pm 0.08$  kbar,  $97.4 \pm 1.5$  C. It might be recalled that similar bounded phases have been observed before in the case of smectic A, (14 – 16) smectic C(17) and cholesteric phases. (12, 18)

The P-T diagram of BH7 is exactly similar to that of BHS. But since the range of the mesophase at atmospheric pressure is larger (5.8 C) than that of BH8 (3.6 C), the triple point is at a higher pressure, viz.,  $2.96 \pm 0.08$  kbar,  $116.5 \pm 1.5$  C. Another interesting and rather unusual feature curve towards the temperature axis whereas the P-T boundaries for the majority of liquid crystal systems composed of rod like molecules (with the exception of a few highly ordered smectics (19)). Have the curvature towards the pressure axis. In other words, for the disc like mesogens, the  $dT/dP$  increases with increase of pressure. Quantitative studies of V and H as functions of pressure are required before the significance of this can be fully appreciated.

The initial values of  $dT/dP$  for the solid – mesophase and mesophase – isotropic transitions are respectively 9.3 C/kbar and 6.0 C/kbar for BH7 and 8.8 C/kbar and 6.6 C/kbar for BH8.

c) Benzene-hexa-n-nonanoate

This compound exhibits a monotropic mesophase at atmospheric pressure at 76.6 C, the melting temperature being 80.4 C. Figure 8 shows the raw DTA traces taken at different pressures. At atmospheric pressure (or very close to it in the high pressure set up) the solid directly transforms into the isotropic liquid in the heating mode as seen from figure 8b, while the isotropic-mesophase and mesophase-solid transitions are clearly resolved in the cooling mode (figure 8a). As the pressure is increased, the mesophase appears in the heating mode also. The nature of the transition changes from monotropic to enantiotropic character even at very low pressures. Experiments

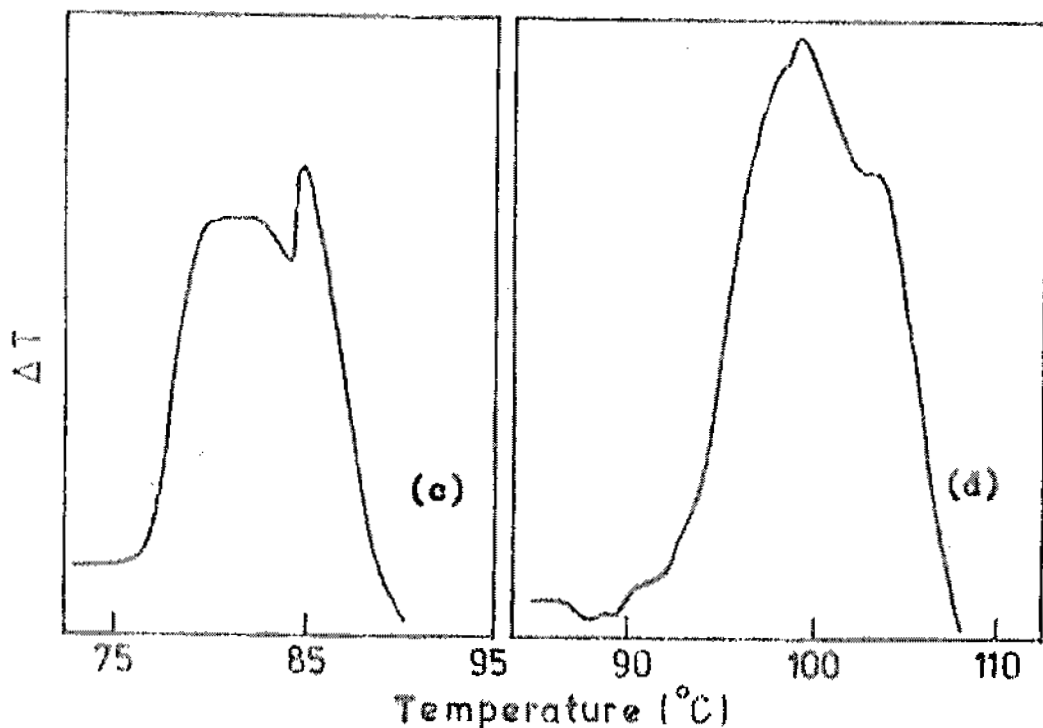
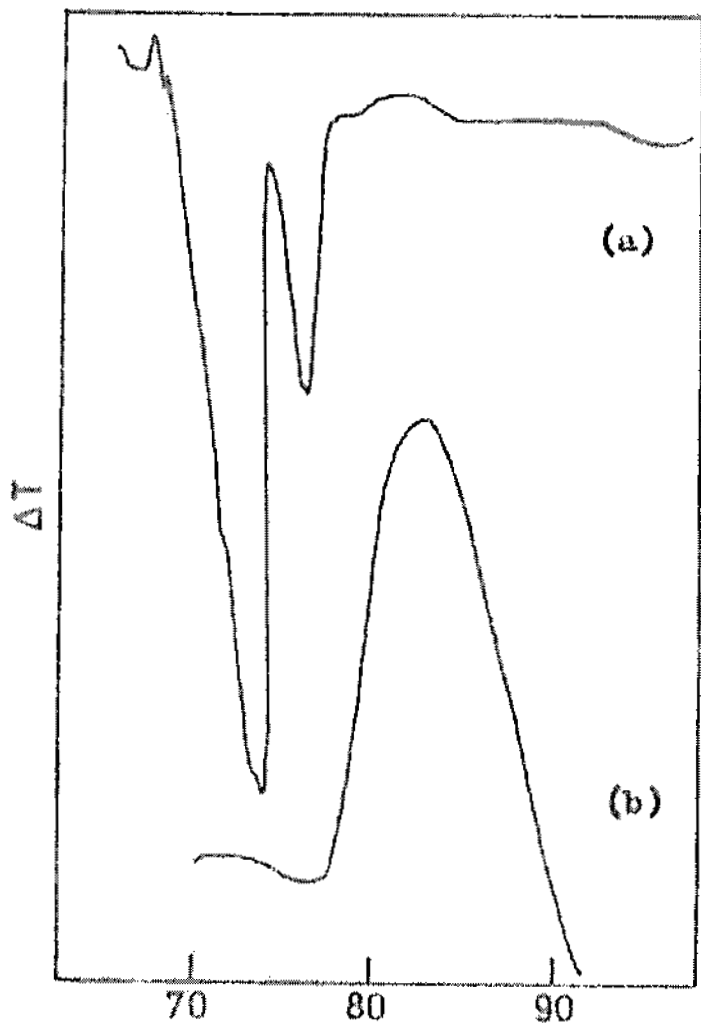


**Figure 8:** Raw DTA traces of BH9 (a) showing monotropic solid-mesophase transition, and (b) showing solid-isotropic transition at atmospheric pressure. (c) at a pressure of 174 bars, (d) at a pressure of 1.3 kbars.

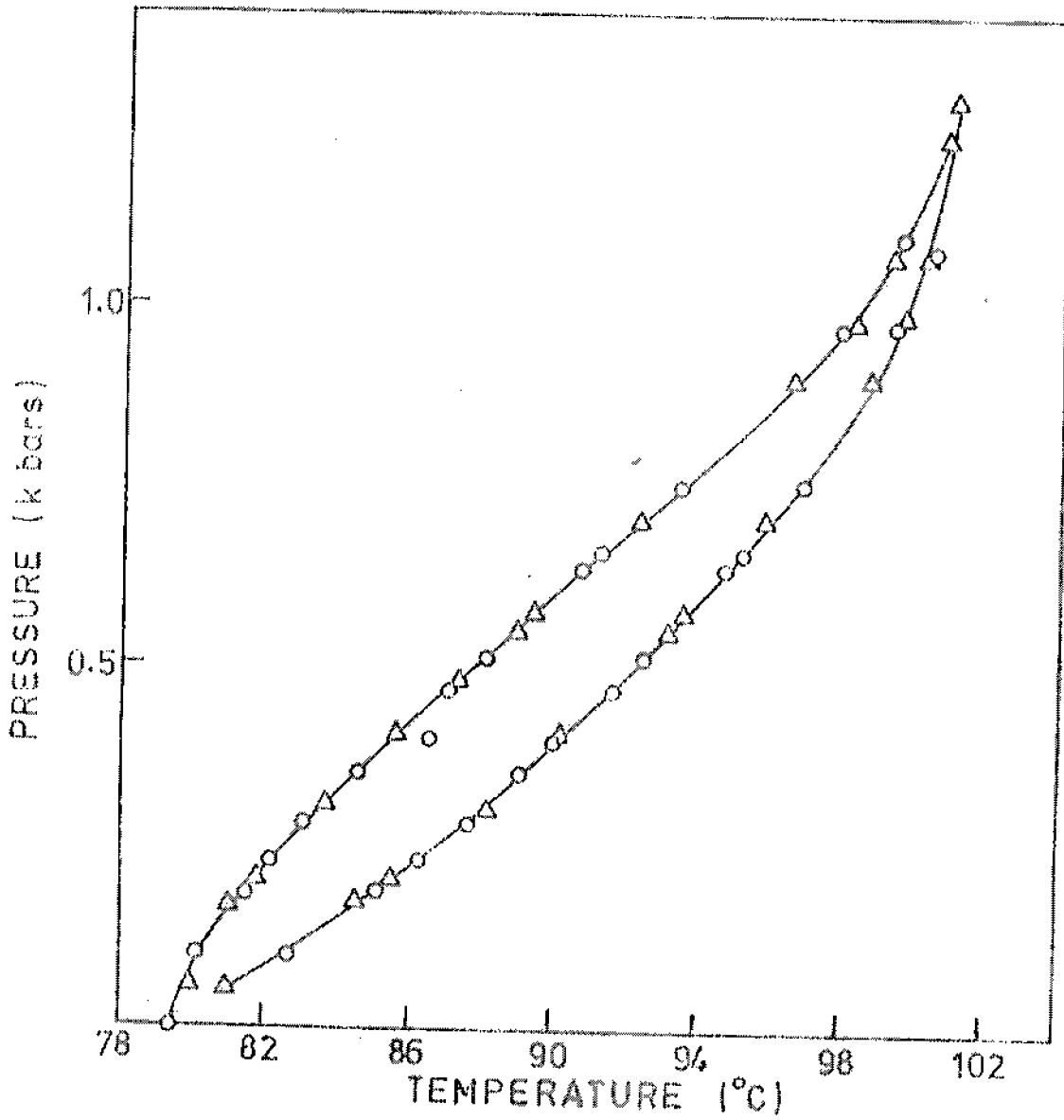


**Figure 9:** Phase diagram of benzene-hexa-n-nonanoate  
 The  $\Delta$  and  $\circ$  represent two independent set  
 of measurements.

conducted with two different cells show that enantiotropic solid-mesophase transition on application of even small pressures, viz., 104 bars and 62 bars. Figure 8c shows the raw DTA traces taken at a pressure of about 170 bars, wherein the solid-mesophase and mesophase-isotropic transitions are clearly separated during the heating mode with increase of pressure, the range of the mesophase decrease with increase of pressure and finally the two transition merge into single on around 1.3 kbar as seen from figure 8d. the data for the two sets of measurement are given in table V and are plotted in figure 9. The solid-mesophase-isotropic triple point is at  $1.3 \pm 0.08$  kbar,  $101 \pm 1.5$  C. As far as we are aware of this is the only case wherein the same compound exhibits the monotropic-enantiotropic change as well as the bounded phase. It is also seen from the figure 9 that both the solid-mesophase and mesophase-isotropic phase boundaries curve towards the temperature axis beyond a pressure of about 600 bars. Since the mesophase had formed even at the first pressures studied, the lower pressure triple point, i.e., the exact pressure at which the monotropic-enantiotropic change in the nature of the transition could not be located accurately. That portion of the curve below 62 bars is left blank in the phase diagram. The  $dT/dP$  values have been evaluated by taking linear portions of the experimental curves very close to atmospheric pressure points. The values can be obtained are 7.7 C/kbar and 22.7 C/kbar for the solid - mesophase and mesophase - isotropic transitions respectively.

#### 4. $dT/dP$ and $\Delta V$ for the homologues

The  $dT/dP$  values obtained from experimental phase diagrams for various transitions are tabulated in table VI. Using these values and the  $\Delta H$  values at atmospheric pressure (given in table I), the volume change  $\Delta V$  at the transitions have been calculated from Clausius - Clapeyron equation. These values are also given in table VI.

The following interesting features are observed:

- (i) The  $dT/dP$  for the solid - isotropic (or solid - mesophase) is roughly the same for all the compounds, about 8 C/kbar. This behaviour is reminiscent of the observation of Feyz and Kuss (20) for melting transitions of 28 compounds belonging to five homologous series, wherein the  $dT/dP$  is roughly the same, about 28.5 C/kbar.

- (ii) For compounds which exhibit mesophases even at atmospheric pressure, viz., BH7 and BH8, the  $dT/dP$  for the mesophase – isotropic transition is also the same, around 6 – 7 C/kbar. This value is rather small compared to the  $dT/dP$  values that are normally observed for the mesophase – isotropic transitions in rod like systems (where usually the values range between 35 – 45 C/kbar)
- (iii) On the other hand, when the mesophase is induced by pressure, the  $dT/dP$  value of the pressure induced phase – isotropic transition increases considerably. For instance these values are 14.8 C/kbar and 22.7 C/kbar for BH6 and BH9 respectively.
- (iv) The volume change associated with all the transitions are quite high, which is not surprising considering drastic structural changes associated with these transitions. In the case of BH9,  $V$  has been calculated assuming that  $H$  for the solid – mesophase and mesophase – isotropic transitions to be the same as those obtained for the monotropic phase from DSC measurements at atmospheric pressure. No conclusions regarding any systematic behaviour of  $V$  can be obtained from these calculations.

**TABLE - I**

**TEMPERATURES AND HEATS OF TRANSITION**

Compound	Transition		Temperature (C)	Heat of Transition Kcals/mole
BH6	Solid I	Solid II	75.7	3.8
	Solid II	Isotropic	94.5	7.9
BH7	Solid	Mesophase	81.2	7.6
	Mesophase	Isotropic	87.0	5.3
	Isotropic	Mesophase	83.5	
BH8	Solid	Mesophase	79.8	10.7
	Mesophase	Isotropic	83.4	4.5
	Isotropic	Mesophase	81.8	
BH9	Solid	Isotropic	80.4	16.7
	Isotropic	Mesophase	76.6	3.4

**TABLE - II****Transition temperatures of BH6 as a function of pressure**

<b>Solid - II - Solid - I</b>		<b>Solid - I - Mesophase ( Pressure induced )</b>		<b>Solid - I ( or mesophase ) - Isotropic</b>	
<b>Pressure in kbars</b>	<b>Temperature in °C</b>	<b>Pressure in kbars</b>	<b>Temperature in °C</b>	<b>Pressure in kbars</b>	<b>Temperature in °C</b>
0.035	76.5			0.035	96.1
0.100	77.9			0.100	96.4
0.116	78.2			0.124	96.6
0.178	79.25	0.182	97.0	0.185	97.7
0.220	80.0	0.220	97.5	0.220	98.6
0.267	80.8	0.267	98.25	0.267	100.0
0.317	81.6	0.325	99.0	0.325	101.6
0.390	82.9	0.398	100.2	0.398	103.2
0.464	84.2	0.471	101.4	0.471	105.0
0.503	84.8	0.487	101.8	0.487	105.3
0.526	85.3	0.530	102.5	0.530	106.2
0.715	86.6	0.717	106.0	0.719	109.2
0.947	91.75				



**Table – III****Transition temperature of BH7 as a function of pressure**

<b>Solid – Mesophase</b>		<b>Mesophase – Isotropic</b>	
<b>Pressure in kbars</b>	<b>Temperature in °C</b>	<b>Pressure in kbars</b>	<b>Temperature in °C</b>
0.278	81.0	0.278	87.0
0.500	82.0	0.500	90.5
0.715	86.5	1.063	96.0
1.063	90.5	1.443	99.0
1.443	96.0	1.973	103.0
1.973	99.0	2.264	108.0
2.264	102.5	2.970	116.5
2.706	109.5		
2.494	107.0		
2.970	116.5		
3.138	125.0		

**Table - IV****Transition temperature of BH8 as a function of pressure**

<b>Solid - Mesophase</b>		<b>Mesophase - Isotropic</b>	
<b>Pressure in kbars</b>	<b>Temperature in °C</b>	<b>Pressure in kbars</b>	<b>Temperature in °C</b>
0.108	80.1	0.108	84.3
0.209	81.0	0.209	85.0
0.236	81.75	0.236	85.2
0.329	82.25	0.329	85.8
0.427	83.2	0.414	86.6
0.441	83.2	0.441	86.8
0.475	83.6	0.475	87.1
0.503	84.0	0.615	88.4
0.603	85.0	0.785	90.3
0.615	85.25	0.877	91.25
0.792	87.1	1.109	93.8
0.874	88.0	1.301	95.8
0.947	88.9	1.313	95.9
1.047	90.4	1.386	96.8
1.109	91.4	1.419	97.4
1.306	94.8	1.596	101.8
1.386	96.8	1.851	108.75
1.419	97.4		
1.596	101.8		
1.851	108.75		

Table - IV

Transition temperatures of BH9 as a function of pressure

Solid - Mesophase		Mesophase - Isotropic	
Pressure in kbars	Temperature in °C	Pressure in kbars	Temperature in °C
0.062	80.0	0.062	81.0
0.104	80.2	0.104	82.6
0.174	81.0	0.174	84.5
0.186	81.5	0.186	85.0
0.209	81.7	0.209	85.5
0.236	82.1	0.236	86.2
0.286	83.0	0.286	87.5
0.313	83.6	0.313	88.1
0.352	84.5	0.352	89.0
0.406	85.6	0.406	90.1
0.468	87.0	0.468	91.5
0.479	87.4	0.479	91.7
0.514	88.0	0.514	92.4
0.545	88.8	0.545	93.0
0.568	89.3	0.568	93.5
0.634	90.7	0.634	94.6
0.653	91.1	0.653	95.1
0.703	92.25	0.703	95.8
0.750	93.4	0.750	96.7
0.897	96.5	0.897	98.7
0.970	97.8	0.970	99.4
0.978	98.1	0.978	99.6
1.067	99.2	1.067	100.2
1.229	100.7	1.229	100.7
1.279	101.0	1.279	101.0

**TABLE – VI**

**dT/dP and AV values for the BH<sub>n</sub> alkanooates (BH6 – BH9)**

<b>Compound</b>	<b>Transition</b>	<b>dT/dP in C/kbar</b>	<b>AV (cm<sup>3</sup> /mole)</b>
BH6	Solid – I ---- Solid II	17.4	7.93
	Solid II ---- Isotropic	6.1	5.53
	Solid II ---- mesophase	6.8	--
	Mesophase ---- isotropic	14.8	--
BH7	Solid ---- mesophase	9.3	8.30
	Mesophase ---- Isotropic	6.0	3.69
BH8	Solid ---- mesophase	8.8	11.21
	Mesophase – Isotropic	6.6	3.54
BH9	Solid – mesophase	7.7	15.28
	Mesophase – Isotropic	22.7	9.25

**References :-**

1. J.D. Brooks and G.H. Taylor, Carbon, 3, 185 (1965).
2. S. Chandrashekar, B.K. Sadashiva and K.A. Suresh, Pramana, 9, 471 (1977).
3. S. Chandrashekar, B.K. Sadashiva, K.A. Suresh, N.V. Madhusudana, S.Kumar, R. Shashidhar and G. Venkatesh, J. de physique, 40, C3-120 (1979).
4. Nguyen Huu Tinh, C.Destrade and H. Gasparoux, phys. lett., 72A, 251 (1979)
5. A. Queguiner, A Zann, J.C. Dubois and J. Billiard ( submitted to phys. Rev.)
6. A.M. Levelut, J. de phys. Lettres, 40, L-81 (1979).
7. C. Destrade, Nguyen Huu Tinh, H.Gasparoux, J. Malthete, A.M. Levelut ( submitted to J de Physique).
8. A.M. Levelut, Proceedings of the International Liquid Crystals Conference, Bangalore, December 1979, Ed. S. Chandrashekar, Heyden, London, p.21 ( 1980).
9. S. Chandrashekar, R.Shashidhar and N. Tara Mol. Cryst. Liquid Cryst., 10, 337 (1970); ibid, 12, (1971); S. Chandrashekar and R. Shashidhar, Mol. Cryst. Liquid Cryst., 16., 21 (1972).
10. S. Chandrashekar, S. Ramaseshan, A.S. Reshamwala, B.K. Sadashiva, R. Shashidhar and V. Surendranath, Proceedings of the International Liquid Crystals Conference, Bangalore, December 1972, Ed. S. Chandrashekar – Pramana Suppl. 1, p.117.
11. R. Shashidhar, Mol. Cryst. Liquid Cryst., 43, 71 (1977).
12. P.E. Cladis, D. Guillon, W.B. Daniels and A.C. Griffin, Mol. Cryst. Liquid Cryst. Lett., 56, 89 (1979).

13. J. Billiard and B.K. Sadashiva, *Pramana*, 13,309 (1979).
14. W.J. Lin, P.H. Keyes and W.B. Daniels, *Phys. Lett. A*, 49, 453 (1974).
15. P.E. Cladis, R.K. Bogardus, W.B. Daniels and G.N. Taylor, *Phys. Rev. Lett.*, 39, 720 (1977).
16. P.E. Cladis, R.K. Bogardus and D. Aadsen, *Phys. Rev. A.*, 18,2292 (1978).
17. R. Shashidhar and S. Chandrashekar, *J. de physique*, 36, C1-49 (1975).
18. P.H. Keyes, H.T. Weston, W.J. Lin and W.B. Daniels, *J.Chem.Phys.*, 63, 5006 (1975).
19. W. Spratte and G.M. Schneider, *Mol. Cryst. Liquid Cyst.*, 51, 101 (1979).
20. M. Feyz and E. Kuss, *Ber, Bunsens. Phys. Chem.*, 78,834 (1974).
21. S. Chandrashekar and R. Shashidhar, 'High Pressure Studies on Liquid Crystals' in *Advances in Liquid Crystals*, 4, 83 (1979).

## CHAPTER - VII

### NEW HIGH PRESSURE OPTICAL CELL FOR LIQUID CRYSTALS.

#### 1. INTRODUCTION

All the work discussed so far in the previous chapters was conducted using the high pressure DTA cell. Although, highly successful in detecting even faint first order transitions, it has a drawback in that it cannot be used to detect and continuously track a 'truly' second order transition as a function of pressure. It is true that the DTA cell was used to study the tricritical behaviour of SCB (chapter IV), wherein the A-N transition which was first order at atmospheric pressure was found to become second order ( or nearly so) at about 2.7 kbar. This experiment was possible because to start with one was studying a transition which had a reasonable transition enthalpy and hence could be easily detected by the DTA probe. With increase of pressure the heat associated with the transition decreased. However, by doing experiments at small intervals of pressure, it was possible to locate with reasonable accuracy, the pressure at which the transition became practically second order and the run showed only a change of slope. On the other hand, when one is dealing with a continuous transition like smectic C - smectic A (C-A) transition, it is very difficult to detect it in the first instance and almost impossible to study its behaviour as a function of pressure.

Also while studying the polymorphism of smectics ( see chapter V), which involve a C-A transition, a need arose to do experiments using an optical transmission cell. As discussed earlier ( chapter I ) several types of optical transmission cells (1-4) have already been used for liquid crystal study. However, all of the are designed as direct pressure transmission cells, i.e., invariably in all these cases a hand pump was used to pump the hydraulic fluid directly into the optical cell, thereby pressurizing the sample contained within. Although convenient, this technique cannot be used for pressures beyond 3 to 4 kilobars, since it is very difficult to deal with such high line pressures. It was therefore thought worthwhile to design and fabricate a new type of optical cell which can be incorporated within the 200 ton hydraulic press used by us. This cell, though relatively simple in its design, has certain unusual features which warrant a description in detail. In this chapter we shall give the constructional details of the cell, its working as well as its calibration.

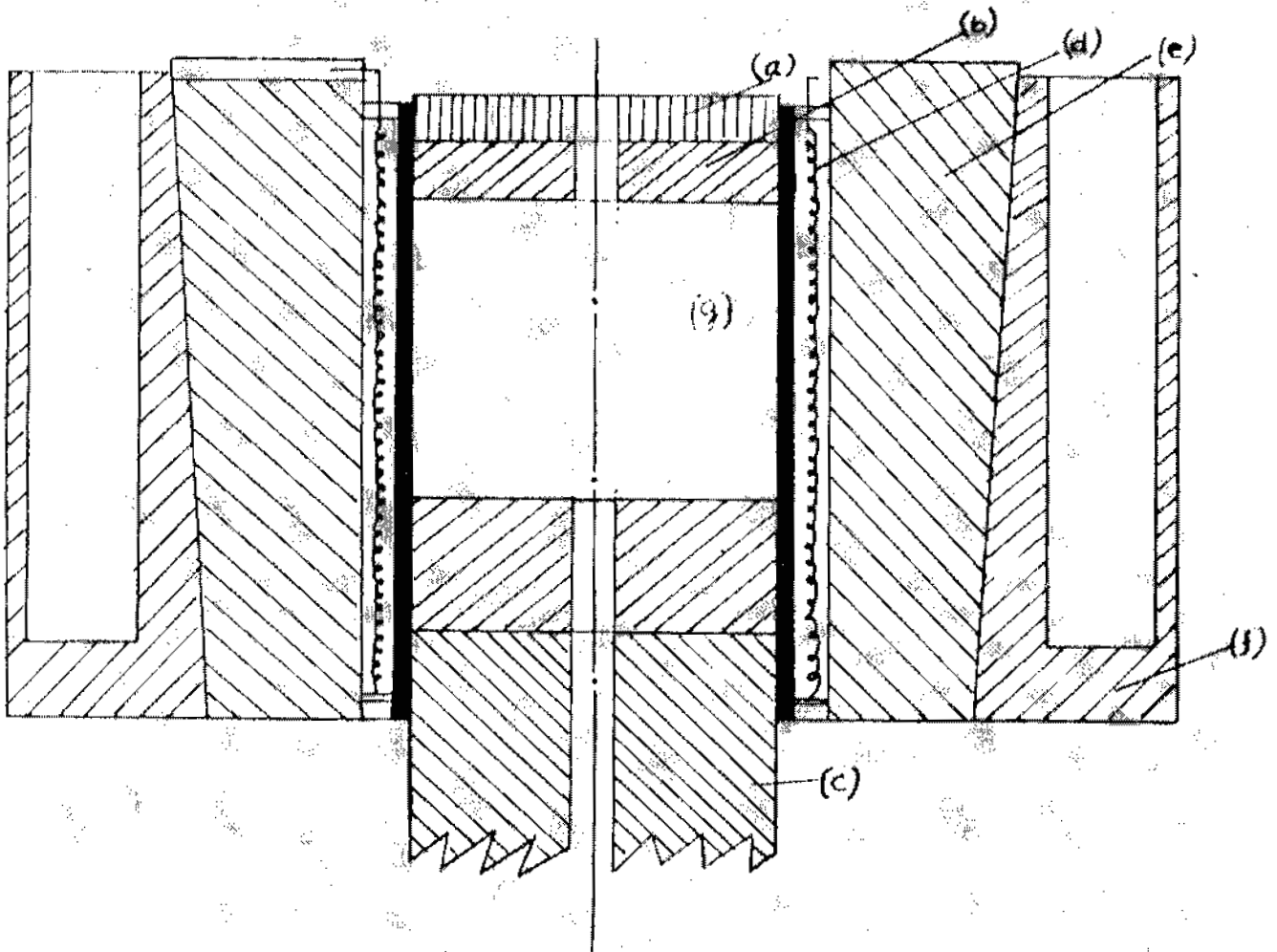


Figure 1: Schematic diagram of the optical cell.  
 (a) MS disc (b) HC-HC die (a) Piston  
 (d) heating coil (e) end load plate.  
 (f) cooling jacket (g) sample cell assembly.

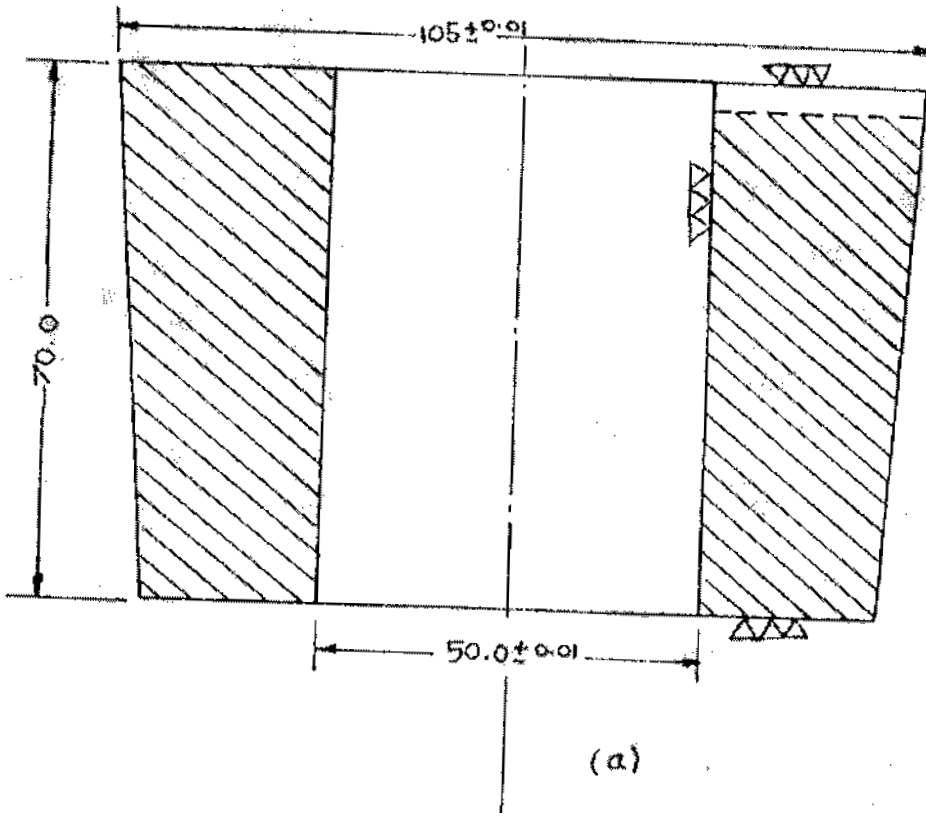
## 2. Description of the experimental set up

### a) Pressure vlate and its accessories

The experimental set up used is given schematically in figure 1. ( The details of the sample cell not shown here will be discussed in the next section). Although basically the press in its entirety as described in Chapter II was for these experiments also, the pressure plate with heating assembly and the end load plate along with the cooling jacket had to be modified to suit the requirements.

The core of the pressure plate consists of a HC-HC die ( figure 1b) heat treated to a hardness of RC 50-55. The internal diameter of this is carefully ground and lapped to match the outer diameter of the piston which has an axial through hole of about 5mm to facilitate observation. Figure 2 shows the scale drawing of the pressure die enclosed by the heating assembly. There is a 2.3 mm hole on one side of the pressure die ( figure 2b) going into a depth of about half the length of the pressure die, through which a thermocouple junction ( which is aligned so that it is well in line with the sample) enclosed in a ceramic tube can be inserted. The heating assembly consists of a brass cylinder ( figure 2e) in which nichrome wires ( figure 2d) are wound, the windings being insulated from the pressure die and the brass cylinder using thin sheets of mica ( figure 2c). Two rings, ( figure 2g) one on top and the other at the bottom of the heater, help to firmly anchor the heating jacket to the pressure die. The pressure die with the heater slides into an end load plate ( figure 3a) made out of EN – 24 which is heat treated to RC 38-40. It has a 1 ½ single taper on the outside and has three 3mm wide slots on the top surface ( figure 3b) through which heater as well as thermocouple leads can be cooling jacket ( figure 4a) made out of aluminium ( which has a matching internal taper) the press fitting being carried out at a pressure of about 200 bars. By suitably scooping out material from the jacket and by closing the top of





SLOTS: 5 mm wide  
9 mm p.c.f.

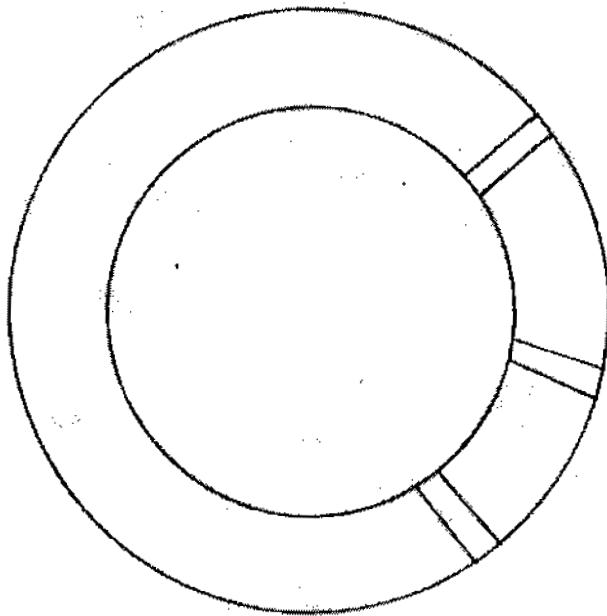


Figure 3: (a) End load plate, (b) Gross section of the end load plate showing slots to take out heater leads and thermocouple leads.

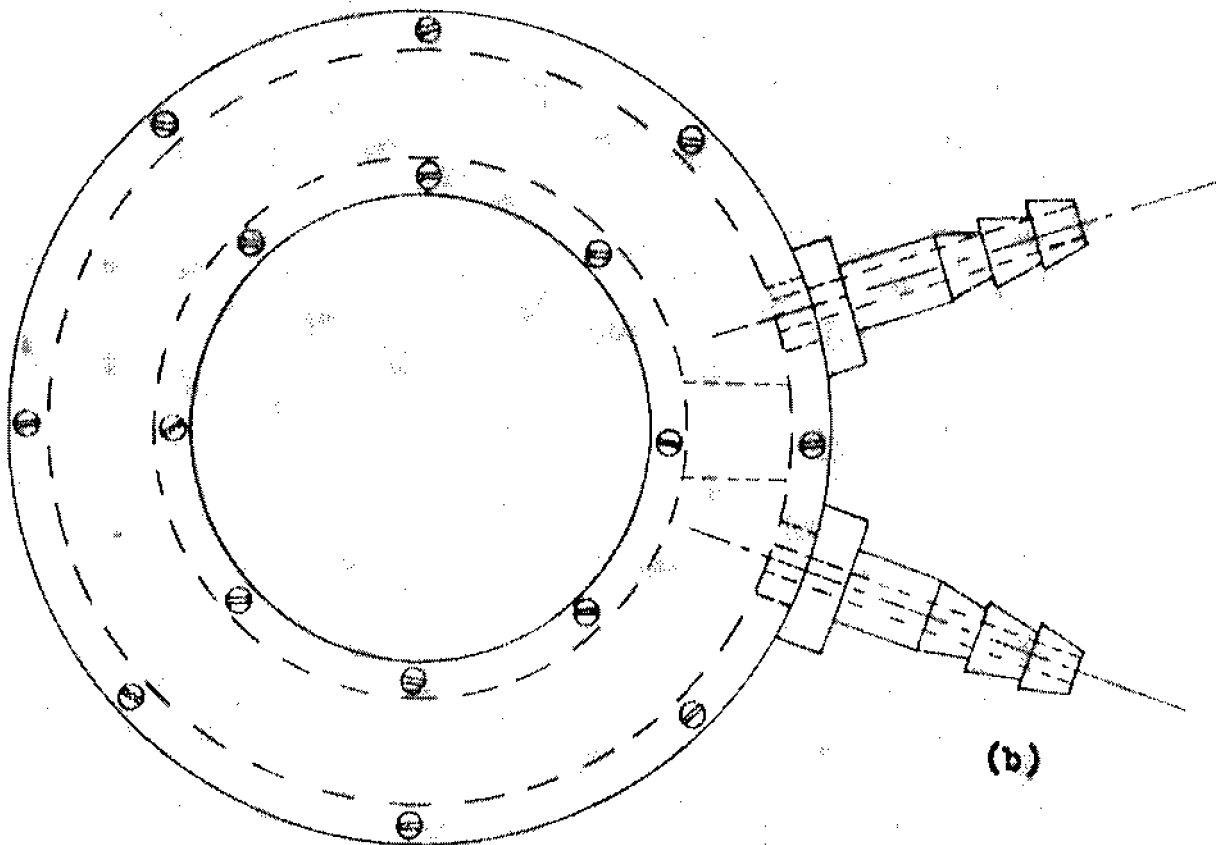
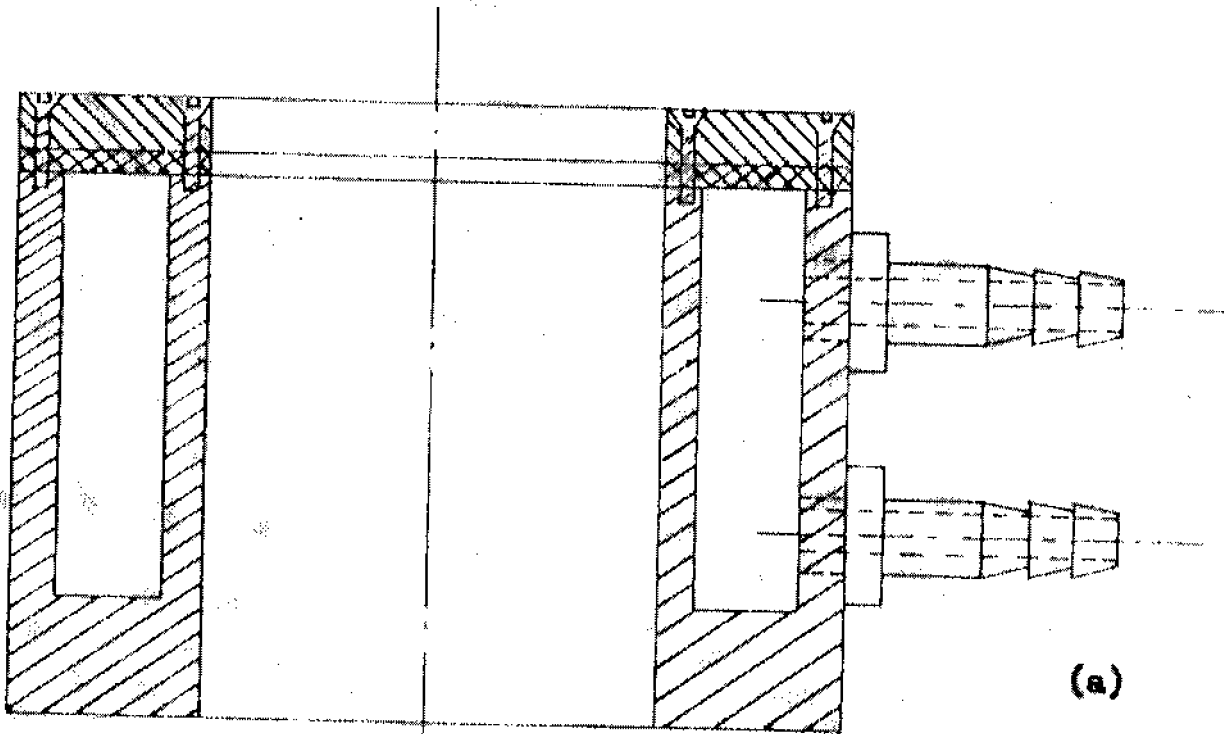


Figure 4: (a) Aluminium cooling jacket (b) Cross section of the jacket showing the inlet and outlet for water.

the jacket with an aluminium lid provided with two sets of screws, water can be passed into the jacket without any leaks. Nozzles are so located ( fig 4b) that water passes through practically the entire circumference of the jacket, thus making the cooling system very efficient.

#### b) Sample Cell

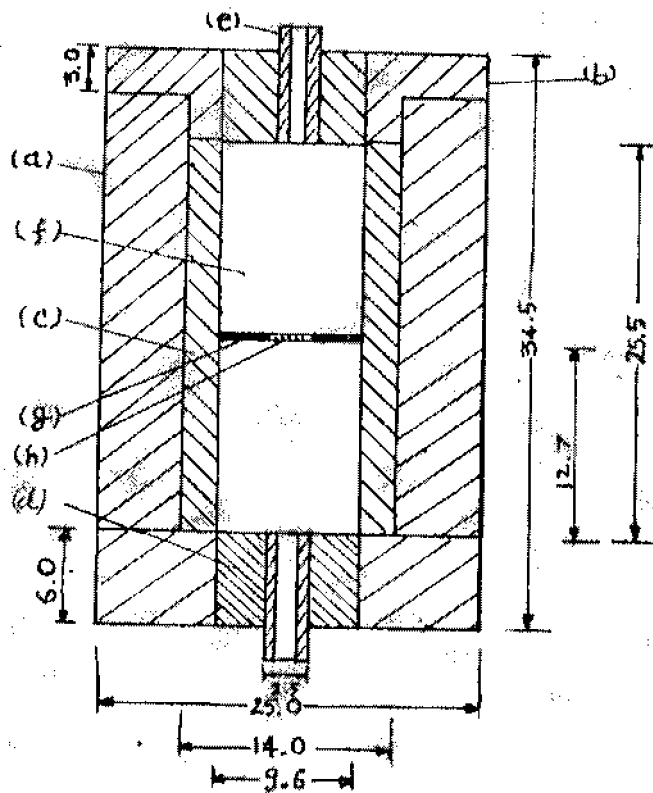
It is well known that the most useful material for use as a window in an optical high pressure cell is sapphire. Sodium Chloride windows have been used in conjunction with piston cylinder apparatus for high pressure studies on solids. However, in the case of liquid crystals there are certain special difficulties.

(i) the sample may react with sodium chloride or other pressure transmitting medium like silver chloride or boron nitride.

(ii) the sample must be contained in the cell assembly ( without leaking) in the liquid crystal and isotropic phases.

Initial experiments were conducted by keeping large sapphire discs ( 25mm diameter), directly on the piston and compressing the sample between the two sapphire discs. However, invariably sapphire windows used to crack indicating a non uniform stress falling on the surface of the windows. Although sapphire is known to be extremely strong under compressive stress (300,000 psi), it evidently could not stand any non-uniform stresses. After trying out various possibilities, finally a cell assembly was arrived at whose schematic diagram is shown in fig 5.

The sample is enclosed inside an aluminium gasket ( 25 microns thick ) ( figure 5g) which is punched out of a flat sheet and is sandwiched between two sapphire rods ( Insaco Inc. USA) as shown in fig 5f. The sapphire assembly, having a diameter of 9mm and length of 12.5 mm, slides into a pyrophyllite sleeve ( fig 5c). This entire system then slides into a teflon cup ( fig 5a) and is closed on the top by a Teflon cap (fig 5b). Both the cup and the cap have axial holes for optical observations. A major problem that was encountered during the preliminary experiments was that the Teflon surrounding the holes flowed under pressure, thereby closing the hole beyond a certain pressure. This was prevented by having two pyrophyllite discs ( fig 5d) with Ms sleeves ( fig 5e) on either side. Two purposes are served by the sleeves. Firstly, they prevent cracking of the pyrophyllite disc near the hole. Secondly, since they are so machined to have an outer diameter as to slide easily into the holes of the HC-HC discs covering either side of the



1-4  
1-4

**Figure 5:** Assembly of the sapphire cell  
 (a) Teflon body (b) Teflon cap  
 (c) Pyrophyllite sleeve  
 (d) Pyrophyllite disc  
 (e) MS sleeve (f) Sapphire rods  
 (g) Gasket (h) Sample

same time, by a combination of teflon and pyrophyllite system, transmit pressure to the sample through sapphire without breaking the windows,

### 3. Working of the cell

#### (a) Method of pressure transmission to the cell

After assembling the cell as discussed in the previous section, it is buffered on both sides by two HC-HC discs (figure 1b) which have central holes for observation, and the cell with the HC-HC discs was placed on the piston inside the pressure die. Over the top HC-HC disc is placed an MS disc (figure 1a) which essentially serves to even out any non smoothness of the surface of HC-HC. The thickness of the MS disc is so adjusted that about 2 mm of it projects out of the pressure die. To start with, the end load plate is raised till it makes contact with the top platen pad. After fixing up an end load pressure of about 30 bars, the piston is now moved slowly (see chapter Sf for the details of operation of the press). The sample cell assembly placed on the piston is hence raised till the protruding MS disc comes into contact with the top platen pad. Any further raising of the piston now generates a compression on the cell, which in turn is transmitted to the sample enclosed between the sapphire windows through the teflon and pyrophyllite system.

#### (b) Pressure measurement and calibration

Since the 200 ton hydraulic press has already been checked for linearity at various pressures, using the manganin

gauge (see, chapter XI), same corrections for relative pressures will hold good here; To determine the actual pressures experienced by the sample, a compound whose phase diagram is known, 4,4'-di-n-heptyloxyazoxybenzene (HOAB) was studied and the phase diagram of this was compared with those obtained earlier. The cell pressure was evaluated by considering the difference in areas of the sapphire and the piston. The pressure evaluated in this way agreed extremely well with the phase diagram obtained from DTA experiments showing thereby the validity of the calculation of the pressure in this manner.

(c) Determination of transition temperatures under pressure

Considering that the optical path length involved is very large (about 1.5 metres), the obvious choice for the light source was a Helium-Neon laser (Spectra Physics). By careful horizontal as well as vertical alignment of a mirror inclined at 45°, the laser beam was made to go right at the centre of the sample cell. The light transmitted by the sample was collected and measured by a photo transistor (Motorola - MRD 300). Since adjustment of the sample cell was not possible, the photocell mount was provided with facilities for coarse as well as fine adjustments in two mutually perpendicular directions. The output of the photo transistor was fed to the y axis of an x-y recorder (Ricken-Denshi F-43P), while the temperature to the x-axis. Initially, by keeping the cell assembly without the sample, on

a fully retracted piston, the mirror position as well as the photo transistor position were adjusted to get a maximum output. Keeping the laser on, the piston was slowly raised till the cell made contact with the top platen pad, at which point also, it was ascertained that the output was the same as before, showing thereby, that the beam was exactly parallel to the direction of movement of the piston. Having thus ascertained the adjustment of the piston, the sample was then sandwiched between the sapphire windows and experiments were conducted by varying the temperature of the sample at the rate of 2-3° C/min. at each pressure. Whenever there was a phase transition, the recorder pen showed a sharp change of the base line. The transition temperature could in this way be detected to an accuracy of  $\pm 1^\circ$  C.

This cell can also be used to study the various other properties like the variation of the birefringence and hence the order parameter, <sup>(8)</sup> light scattering, variation of the pitch of a cholesteric, <sup>(9-11)</sup> pretransition effects in the vicinity of cholesteric-smectic A transition, etc. as a function of pressure. Also, this cell facilitates the microscopic observation of a thin layer of the liquid crystal sample under pressure so that the pressure induced phases can be identified from the optical textures exhibited by them. Experiments are in progress in this direction with the new optical cell.

References

1. G.A.Hullet, Z. Phys. Chem., 28, 629 (1099)
2. J. Robberecht, Bull. Soc. Chim. Belg., 47, 597 (1938).
3. P.H.Keyes, H.T.Weston and WB. Daniels, Phys.Rev.Lett., 31, 628 (1974).
4. M. Feyn and E. Kuss, Ber Bunsenges. Phys. Chem., 78, 834 (1974).
5. R.A.Fitch, T.E.Slykhouse and H.G.Drickamer, J.Opt.Soc.Amer., 1015 (1975).
6. H.G.Drickamer, in Progress in Very High Pressure Research, (Eds. F.P.Bundy, W.R.Hibbard and H.M.Strong), Wiley, New York (1961), Rev. Sci. Inst., 32, 212 (1961).
7. R. Wilkinson, 'Molecular and Solid State Spectroscopy Report', 1959-60.
8. S. Chandrasekhar and N.V.Madhusudana, J.Physique, 30, C4-24 (1969).
9. P. Pollmann and H. Stegemeyer, Chem. Phys. Lett., 20, 87 (1973).
10. P. Pollmann and H. Stegemeyer, Ber. Bunsenges, Phys. Chem., 78, 843 (1974).
11. S. Chandrasekhar and B.R.Ratna, Mol. Cryst. Liquid Cryst., 35, 109 (1976).